Journal of Organometallic Chemistry, 471 (1994) 201–209

Synthesis, structure, and oxidation-induced dimerization of a chelating bis(phosphite) Ruthenium carbonyl

Bahram Moasser, Christopher Gross and Wayne L. Gladfelter

Department of Chemistry, University of Minnesota, Minneapolis, MN 55455 (USA)

(Received March 2, 1993; in revised form September 27, 1993)

Abstract

The novel bis(phosphite) compound Ru(bbmb)$(CO)_3$ (**1**) {bbmb: 2,2′-bis[(1,1′-biphenyl-2,2′-diyl)phosphite]-3,3′-di-t-butyl-5,5′-dimethoxy-1,1′-biphenyl} was synthesized by the high pressure reaction of $Ru_3(CO)_{12}$ with bbmb, and fully characterized by combustion, spectroscopic, spectrometric and structural analysis. The structure of **1**, as determined by X-ray diffraction, is a nearly perfect trigonal bipyramid with the bbmb ligand coiled about Ru in an overall C_2 fashion. Reaction of **1** with $[Cp_2Fe][PF_6]$ gave $[Ru_2(\mu\text{-bbmb})_2(CO)_6][PF_6]_2$ (**2**) whose formulation is based on combustion and spectroscopic analysis. It is shown that **2** contains a pair of bridging bbmb ligands. The significance of **1** in relation to structure-activity in the regioselectivity of the hydroformylation reaction is discussed. Formation of **2** from **1** is addressed in the context of the reactivity of pentacoordinate radical cation complexes.

Key words: Ruthenium; Bis(phosphite); Carbonyl; Crystal structure

1. Introduction

Although chelating phosphine complexes have been extensively studied [1], only recently have reports describing bis(phosphite) complexes and their catalytic activity towards hydroformylation [2] and hydrocyanation [3–5] appeared. Ready and inexpensive preparation of electronic and steric assortments of the relatively stable bis(phosphite) ligands makes them convenient for the mechanistic study of organometallic reactions. Our interest in the reductive carbonylation of nitroaromatics [6,7], and the structure and reactivity of pentacoordinated, 17-electron, metal-centered radicals [8] prompted us to examine the potential contribution of these ligands to the above chemistry. Here we report the synthesis and characterization of the novel Ru(bbmb)$(CO)_3$ (**1**) {bbmb: 2,2′-bis[(1,1′-biphenyl-2,2′-diyl)phosphite]-3,3′-di-t-butyl-5,5′-dimethoxy-1,1′-biphenyl}, and its oxidative dimerization to $[Ru_2(\mu\text{-bbmb})_2(CO)_6][PF_6]_2$ (**2**) (Scheme 1).

Correspondence to: Professor W.L. Gladfelter.

2. Results

2.1. Ru(bbmb)$(CO)_3$ (1)

The bulky bis(phosphite), bbmb, was synthesized by modification of reported procedures [2]. The oxidative coupling of 3-t-butyl-4-hydroxy anisole to 3,3′-di-t-butyl-2,2′-dihydroxy-5,5′dimethoxy-1,1′-biphenyl was altered slightly to make it more amenable to bench top preparation and gave a typical yield of 56%. Final assembly of the ligand was carried out as described (62% yield) [2]. High pressure reaction of bbmb with $Ru_3(CO)_{12}$ gave pale yellow **1** (34% yield), whose formulation was based on mass spectral data and elemental analysis as well as single-crystal X-ray structural analysis.

The ν(CO) region in the IR spectrum of **1** in CH_2Cl_2, toluene or KBr glass exhibits a sharp absorbance at 1998 cm^{-1} and a broad band at 1964 cm^{-1}. A similar pattern of much lower intensity appears at 2068 cm^{-1} and 2050 cm^{-1}. The ^{13}C NMR and ^{31}P NMR spectra of **1** contain single resonances at δ 207 (due to the metal carbonyls) and δ 189.4, respectively. Noteworthy features of the ^1H NMR spectrum are

0022-328X/94/$7.00
SSDI 0022-328X(93)24220-Y

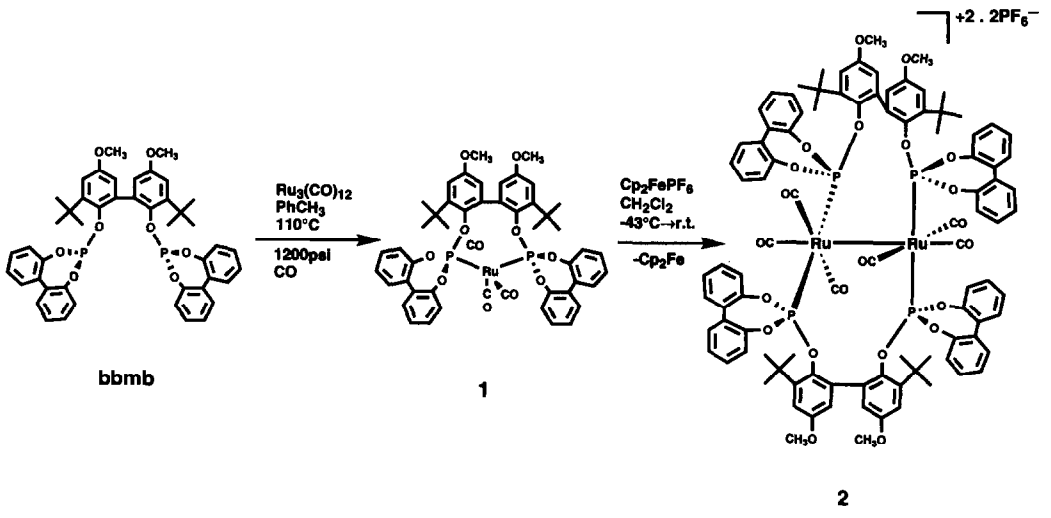

Scheme 1.

singlets at δ 1.52 and δ 3.39 for equivalent pairs of $C(CH_3)_3$ and OCH_3 fragments. The UV-vis spectrum of **1** contains a λ_{max} at 238 nm ($\epsilon = 46{,}673\ M^{-1}\ cm^{-1}$).

An ORTEP diagram of **1** is shown in Fig. 1, and the atom labelling scheme for the bbmb ligand is shown in Fig. 2. Crystallographic data, selected bond distances,

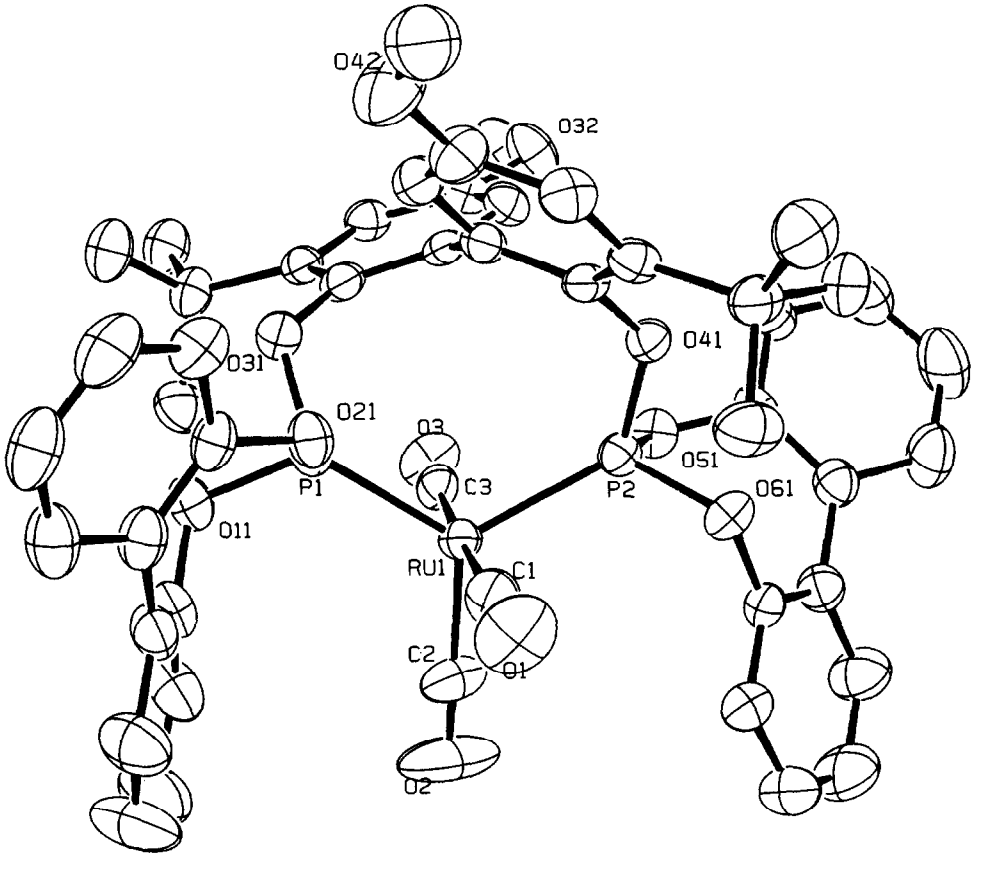

Fig. 1. Molecular structure and heavy atom labelling of (bbmb)$Ru(CO)_3$ (**1**) with thermal ellipsoids shown at 50% level.

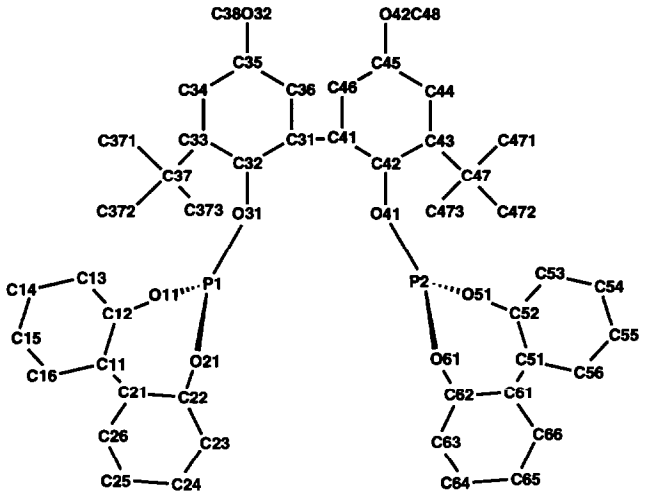

Fig. 2. Atom labelling for the bbmb ligand.

bond angles and atomic coordinates are shown in Tables 1, 2, 3 and 4, respectively. In the crystal structure, **1** exhibits an almost perfect trigonal bipyramidal structure with P(1)–Ru(1)–P(2) angle of 118.98(6)° and rigorous C_2 symmetry about Ru(1)–C(2). A notable feature of the structure of **1** is the C(32)–C(31)–C(41)–C(42) torsion angle of 133.0(5)°. The equatorial C(2)–O(2) bond length is sizably shorter than the apical C(1)–O(1) and C(3)–O(3) bond, reflecting the poorer, relative to CO, backbonding ability of phosphites.

2.2. $[Ru_2(\mu\text{-bbmb})_2(CO)_6][PF_6]_2$ (2)

Oxidation of **1** with ferrocenium hexafluorophosphate gave canary yellow **2** (39% yield). Spectroscopic and combustion analysis allowed us to formulate a structure (see below). The ultraviolet spectrum of **2** exhibits an absorption at $\lambda_{max} = 388$ nm ($\epsilon = 13{,}900$ M^{-1} cm^{-1}) attributed to the formally allowed ($\sigma \rightarrow \sigma^*$) transition of the metal–metal bond. This compares favorably with related compounds: $Ru_3(CO)_{12}$ (390 nm, $\epsilon = 6400$ M^{-1} cm^{-1}) [9]; $Ru_3(PPh_3)_3(CO)_9$ (387 nm, $\epsilon = 12{,}800$ M^{-1} cm^{-1}) [9]; $Ru_2Cp_2(CO)_4$ (265 nm, $\epsilon = 10{,}950$ M^{-1} cm^{-1}, bridged; 330 nm, $\epsilon = 13{,}900$ M^{-1} cm^{-1}, non-bridged) [10]; and $Ru_2[\mu\text{-}(\eta^5\text{:}\eta^5\text{-fulvalene})](CO)_4$ (388 nm, $\epsilon = 1514$ M^{-1} cm^{-1}) [11].

The $^{31}P\{^1H\}$ NMR spectrum consists of a pair of triplets ($J_{av} = 21.5$ Hz) at δ 146.0 and δ 132.1 along with the PF_6^- heptet at δ −143.0 ($J_{PF} = 708$ Hz) in a 2:2:1 ratio. This corresponds well to a calculated spectrum of an AA'BB' spin system (Fig. 3) with $\delta A = \delta A' = 146$ ppm, $\delta B = \delta B' = 132$ ppm, $^3J(P_A\text{–}P_{B'}) = {}^3J(P_{A'}\text{–}P_B) = 23$ Hz, and $^3J(P_A\text{–}P_B) = {}^3J(P_{A'}\text{–}P_{B'}) = 18$ Hz. The requirements for the collapse of the AA'BB' into a pair of triplets ($\rightarrow A_2X_2$), i.e. a large $J(P_A\text{–}P_{A'})$, $J(P_B\text{–}P_{B'})$, $J(P_A\text{–}P_{B'}) = J(P_{A'}\text{–}P_B)$, $J(P_A\text{–}P_B) = J(P_{A'}\text{–}$

TABLE 1. Summary of crystallographic data

Crystal parameters	
Compound	$(bbmb)Ru(CO)_3$
Crystal system	Triclinic
Space group	$P\bar{1}$
Formula	$C_{49}H_{44}O_{11}P_2Ru$
Formula weight (g mol^{-1})	971.89
a (Å)	9.884(4)
b (Å)	14.525(7)
c (Å)	17.16(1)
α (°)	98.05(5)
β (°)	104.64(5)
γ (°)	104.94(3)
V (Å^3)	2247(5)
Z	2
ρ (calcd) (g cm^{-3})	1.436
Temperature (°C)	24
Abs. coefficient (cm^{-1})	4.69
Crystal dimensions (mm)	0.300×0.250×0.250
Transmission factors, max to min (%)	0.84–1.12
Absorption correction applied	Empirical (DIFABS)
Measurement of intensity data	
Diffractometer	Enraf-Nonius CAD-4
Radiation	Mo Kα ($\lambda = 0.71069$ Å)
Monochrometer	Graphite crystal
Program used	TEXAN
Method of structure solution	Direct methods
Scan type	ω–2θ
Scan range (°)	0–49.9
Reflections measured	$h, \pm k, \pm l$
Number of unique reflections	7892
Number of reflections used	5686
Cutoff	2σ
ρ	0.05
R	0.047
R_w	0.050
Error in observation of unit weight	1.13

TABLE 2. Bond distances (Å) for $(bbmb)Ru(CO)_3$ (1)

(a) Metal–ligand			
Ru1–C1	1.923(6)	C1–O1	1.144(6)
Ru1–C2	1.925(6)	C2–O2	1.125(6)
Ru1–C3	1.917(5)	C3–O3	1.147(5)
Ru1–P1	2.277(2)		
Ru1–P2	2.257(2)		
(b) Intraligand			
P1–O11	1.631(3)	C41–C42	1.388(6)
O11–C12	1.388(6)	C42–O41	1.411(5)
C12–C11	1.386(7)	O41–P2	1.613(3)
C11–C21	1.478(7)	P2–O51	1.605(3)
C21–C22	1.390(7)	O51–C52	1.409(5)
C22–O21	1.405(5)	C52–C51	1.389(7)
O21–P1	1.611(3)	C51–C61	1.481(7)
P1–O31	1.611(3)	C61–C62	1.393(6)
O31–C32	1.413(5)	C62–O61	1.398(5)
C32–C31	1.394(6)	O61–P2	1.625(3)
C31–C41	1.502(6)		

TABLE 3. Bond angles and torsion angles in (bbmb)Ru(CO)$_3$ (1)

(a) Metal–ligand			
Ru1–P1–O11	120.5(1)	P1–Ru1–C1	89.4(2)
Ru1–P1–O21	113.0(1)	P1–Ru1–C2	122.8(2)
Ru1–P1–O31	122.2(1)	C3–Ru1–P1	93.5(1)
Ru1–P2–O41	125.3(1)	C1–Ru1–P2	90.9(2)
Ru1–P2–O51	113.1(1)	P2–Ru1–C2	118.2(2)
Ru1–P2–O61	118.3(1)	P2–Ru1–C3	86.7(1)
Ru1–C1–O1	178.6(5)	C1–Ru1–C2	90.0(2)
Ru1–C2–O2	179.1(5)	C3–Ru1–C2	89.3(2)
Ru1–C3–O3	176.1(4)	C1–Ru1–C3	177.0(2)
P1–Ru1–P2	118.98(6)		
(b) Intraligand			
O11–P1–O21	99.4(2)	C31–C41–C42	124.0(4)
P1–O11–C12	115.6(3)	C41–C42–O41	119.0(4)
O11–C12–C11	119.2(5)	C42–O41–P2	126.7(3)
C12–C11–C21	120.8(5)	O51–P2–O61	100.5(2)
C11–C21–C22	123.3(4)	P2–O51–C52	124.1(3)
C21–C22–O21	121.0(4)	O51–C52–C51	120.5(4)
C22–O21–P1	127.5(3)	C52–C51–C61	122.4(4)
O21–P1–O31	103.7(2)	C51–C61–C62	121.4(4)
O11–P1–O31	94.2(2)	C61–C62–O61	118.0(4)
P1–O31–C32	122.6(3)	C62–O61–P2	118.6(3)
O31–C32–C31	118.4(4)	O61–P2–O41	94.9(2)
C32–C31–C41	121.9(4)	O51–P2–O41	100.5(2)
C12–C11–C21–C26	137.7(5)		
P1–O11–C12–C11	78.0(5)		
O11–P1–O31–C32	−133.5(3)		
P1–O31–C32–C31	−65.4(5)		
O31–C32–C31–C41	−14.2(6)		
C36–C31–C41–C42	−56.2(6)		
C52–C51–C61–C66	138.8(5)		
P2–O51–C52–C51	69.2(5)		
O51–P2–O41–C42	140.8(3)		
P2–O41–C42–C41	−68.1(5)		
O41–C42–C41–C31	−7.1(6)		
C32–C31–C41–C42	133.0(5)		

$P_{B'}$), and $J(P_A–P_B) \approx J(P_A–P_{B'})$, can be reasonably met only by structures such as **D** and **E** (Fig. 4), because the likelihood of $^3J(P_A–P_B) \approx {}^3J(P_A–P_{B'})$ in **A** and $^2J(P_A–P_B) \approx {}^3J(P_A–P_{B'})$ in **B** is remote, and **C** has only one P environment. The large $^2J(P_A–P_{A'})$, $^2J(P_B–P_{B'})$ does not allow us to differentiate between **D** and **E**. We prefer structure **E** based on the steric disadvantages of **D**, especially considering the bulk of the bbmb ligand. The small difference in the "*cis*" $^3J(P_A–P_B)$ and the "*trans*" $^3J(P_A–P_{B'})$ must be the consequence of a rather large P–Ru–Ru–P dihedral angle and substantial deviation from planarity in the Ru_2P_4 framework. We propose the structure shown in Scheme 1 for **2** to be in agreement with all available evidence. The ^{31}P NMR spectrum of the product in the reaction solution itself was identical to that of purified material discussed above. This rules out the possibility that another diastereomer was formed.

We have yet to explore the reactivity of **2**, only to note that room temperature CH_2Cl_2, $ClCH_2CH_2Cl$/toluene and more rapidly CH_3CN/toluene solutions of **2** under inert atmosphere decomposed to **1**. Interestingly, KBr pellets containing **2** showed disproportionation to **1** and what is probably Ru(bbmb)$(CO)_2Br_2$ (ν(CO) = 2141 cm^{-1}) [12].

When aliquots were removed from the oxidation of **1** at −78°C and instantly examined by IR, we observed the appearance of new peaks (ν(CO) = 2069, 2109, 2149 cm^{-1}) in the early stages of the reaction. These new peaks were embedded among many arising from starting material and product. Because the solutions removed from the reaction rapidly lost the characteristic green color of the radical cations, and the new resonances were not shifted to high enough energy relative to **1**, we are inclined to attribute this new feature in the IR to a fleeting unbridged dimer (such as **A** or **B**) which is the expected intermediate in the formation of **2**.

3. Discussion

There are only a few structurally characterized bis(phosphite) metal complexes, including Co(pinacop)(η^5-2,4-dimethylpentadienyl), Rh(pinacop)(η^3-2,4-dimethylpentadienyl) {pinacop = $\dot{O}CMe_2CMe_2OPOCMe_2CMe_2OPOCMe_2CMe_2\dot{O}$] [13] and *cis*-Mo$(CO)_4${$(R_2PO)_2Si(Me)R'$} [14]. Reports correlating bis(phosphine) "bite angles" with normal to iso ratios in the hydro-formylation of olefins (which increased with bite angle size) have appeared [15–18]. The robust bbmb ligand, exhibiting a P–M–P angle of 118.98(6)° in **1**, may expose further structure-activity relationships in this area. In fact, the remarkable regioselectivity in Union Carbide's hydroformylation [2] using this ligand is consistant with such a relationship. By comparison of **1** to Ru(P(O-*o*-tolyl)$_3)_2$ $(CO)_3$ and Ru[P$(OCH_3)_3]_2$-$(CO)_3$ (both having *trans* phosphite geometry [19]), it is apparent that bbmb is sterically, not electronically, inclined towards this particular geometry, indeed, overcoming the propensity of d^8 metals to confine the better π-acceptor COs to the equitorial plane [20]. It is therefore likely that the same steric forces should prevail in the d^8 rhodium intermediates of the hydroformylation reaction, leading to species of very similar structure, *i.e.* 120° bite angle.

The major peaks in the ν(CO) region of the infrared spectrum are in accord with predictions based on the solid state structure (with one symmetric and the two asymmetric CO stretches close in energy). The anomalous shadow of lower intensity might be arising from an isomeric square pyramidal geometry. In fact, widening of the P–Ru–P angle to that found in a square-based pyramid while retaining C_2 symmetry would predict the same IR pattern. The *tbp–sqp* transformation

TABLE 4. Positional parameters and isotropic temperature factors for (bbmb)Ru(CO)$_3$ (1)

Atom	x	y	z	B_{eq}
Ru1	0.06372(4)	0.24511(3)	0.20991(2)	2.35(1)
P1	0.2222(1)	0.34987(9)	0.16268(7)	2.53(4)
P2	0.1526(1)	0.15787(9)	0.29787(7)	2.42(4)
O1	0.1090(5)	0.4102(3)	0.3556(3)	6.2(2)
O2	−0.2660(5)	0.2156(4)	0.1575(3)	8.2(2)
O3	0.0080(4)	0.0678(3)	0.0730(2)	4.1(1)
O11	0.1606(4)	0.3993(2)	0.0871(2)	3.0(1)
O21	0.3220(3)	0.4474(2)	0.2314(2)	2.8(1)
O31	0.3377(3)	0.3166(2)	0.1227(2)	2.8(1)
O32	0.3755(4)	−0.0573(2)	0.1170(2)	3.9(1)
O41	0.3243(3)	0.1740(2)	0.3418(2)	2.6(1)
O42	0.7988(4)	0.4830(3)	0.3533(3)	5.7(2)
O51	0.0971(3)	0.0427(2)	0.2590(2)	2.8(1)
O61	0.1077(3)	0.1590(2)	0.3827(2)	2.9(1)
C1	0.0924(6)	0.3495(4)	0.3006(3)	3.8(2)
C2	−0.1443(6)	0.2269(4)	0.1775(3)	4.4(2)
C3	0.0317(5)	0.1362(3)	0.1228(3)	2.8(2)
C11	0.1147(6)	0.5418(4)	0.1488(3)	3.4(2)
C12	0.0620(6)	0.4490(4)	0.0984(3)	3.3(2)
C13	−0.0856(6)	0.4055(4)	0.0573(4)	4.5(2)
C14	−0.1828(7)	0.4559(5)	0.0659(5)	6.1(3)
C15	−0.1339(8)	0.5476(5)	0.1167(5)	7.0(3)
C16	0.0129(7)	0.5898(4)	0.1578(4)	5.2(2)
C21	0.2741(6)	0.5905(3)	0.1862(3)	3.3(2)
C22	0.3722(5)	0.5423(3)	0.2190(3)	2.8(2)
C23	0.5216(6)	0.5886(4)	0.2504(3)	3.6(2)
C24	0.5752(6)	0.6863(4)	0.2511(3)	4.5(2)
C25	0.4816(7)	0.7369(4)	0.2211(4)	4.6(2)
C26	0.3346(7)	0.6898(4)	0.1883(3)	4.2(2)
C31	0.4054(5)	0.1940(3)	0.1915(3)	2.4(1)
C32	0.3530(5)	0.2221(3)	0.1181(3)	2.5(2)
C33	0.3157(5)	0.1604(3)	0.0404(3)	2.5(2)
C34	0.3255(5)	0.0670(3)	0.0411(3)	2.7(2)
C35	0.3669(5)	0.0345(3)	0.1133(3)	2.7(2)
C36	0.4109(5)	0.0999(3)	0.1889(3)	2.8(2)
C37	0.2695(5)	0.1921(3)	−0.0419(3)	3.0(2)
C38	0.3242(6)	−0.1278(4)	0.0425(3)	4.3(2)
C41	0.4772(5)	0.2667(3)	0.2725(3)	2.5(1)
C42	0.4435(5)	0.2542(3)	0.3449(3)	2.4(1)
C43	0.5291(5)	0.3138(3)	0.4218(3)	2.7(2)
C44	0.6476(5)	0.3896(4)	0.4224(3)	3.2(2)
C45	0.6819(6)	0.4061(4)	0.3511(3)	3.5(2)
C46	0.5963(5)	0.3447(4)	0.2758(3)	3.2(2)
C47	0.5007(5)	0.3017(4)	0.5047(3)	3.2(2)
C48	0.898(1)	0.539(1)	0.4201(8)	5.8(4)
C49	0.851(2)	0.504(1)	0.295(1)	5.5(4)
C51	0.0129(5)	−0.0467(3)	0.3560(3)	3.0(2)
C52	0.1032(5)	−0.0291(3)	0.3059(3)	2.8(2)
C53	0.1923(6)	−0.0853(4)	0.2938(3)	3.7(2)
C54	0.1930(7)	−0.1614(4)	0.3337(4)	5.2(2)
C55	0.1049(8)	−0.1809(4)	0.3841(4)	5.6(3)
C56	0.0176(7)	−0.1236(4)	0.3956(4)	4.7(2)
C61	−0.0851(5)	0.0125(4)	0.3673(3)	3.2(2)
C62	−0.0385(5)	0.1137(3)	0.3774(3)	2.7(2)
C63	−0.1287(6)	0.1693(4)	0.3867(3)	3.7(2)
C64	−0.2680(7)	0.1252(5)	0.3885(4)	4.9(2)
C65	−0.3171(7)	0.0257(5)	0.3796(4)	5.7(3)
C66	−0.2272(6)	−0.0297(4)	0.3690(4)	4.7(2)
C371	0.2666(6)	0.1172(4)	−0.1157(3)	3.8(2)
C372	0.3798(6)	0.2896(4)	−0.0402(3)	4.0(2)

TABLE 4 (continued)

Atom	x	y	z	B_{eq}
C373	0.1125(6)	0.2002(4)	−0.0591(3)	4.0(2
C471	0.4632(6)	0.1943(4)	0.5134(3)	4.3(2)
C472	0.6348(6)	0.3590(4)	0.5784(3)	4.6(2)
C473	0.3735(6)	0.3425(4)	0.5120(3)	4.4(2)
H1	−0.1195	0.3415	0.0236	5.3
H2	−10.2842	0.4275	0.0366	7.3
H3	−10.2019	−0.5816	0.1234	8.4
H4	0.0455	0.6530	0.1929	6.3
H5	0.5865	0.5536	0.2713	4.3
H6	0.6778	0.7188	0.2725	5.4
H7	0.5190	0.8047	0.2231	5.5
H8	0.2713	0.7253	0.1662	5.0
H9	0.3028	0.0230	−0.0102	3.2
H10	0.4448	0.0798	0.2387	3.4
H11	0.2231	0.1365	0.0173	5.2
H12	0.3785	−0.1064	0.0064	5.2
H13	0.3364	−0.1879	0.0533	5.2
H14	0.7079	0.4321	0.4736	3.8
H15	0.6189	0.3557	0.2267	3.8
H16	0.9881	0.5250	0.4250	7.0
H17	0.9117	0.6055	0.4172	7.0
H18	0.8666	0.5276	0.4668	7.0
H19	0.9418	0.4907	0.3033	6.5
H20	0.7837	0.4656	0.2441	6.5
H21	0.8654	0.5712	0.2956	6.5
H22	0.2520	−0.0719	0.2587	4.4
H23	0.2543	−0.2005	0.3265	6.2
H24	0.1047	−0.2339	0.4108	6.7
H25	−0.0408	−0.1368	0.4314	5.6
H26	−0.0948	0.2380	0.3919	4.5
H27	−0.3305	0.1634	0.3960	5.9
H28	−0.4138	−0.0048	0.3807	6.8
H29	−0.2628	−0.0984	0.3628	5.7
H30	0.1977	0.0561	−0.1198	4.6
H31	0.2389	0.1395	−0.1651	4.6
H32	0.3615	0.1097	−0.1079	4.6
H33	0.4741	0.2815	−0.0336	4.8
H34	0.3488	0.3093	−0.0905	4.8
H35	0.3845	0.3380	0.0046	4.8
H36	0.1088	0.2461	−0.0151	4.8
H37	0.0865	0.2211	−0.1093	4.8
H38	0.0456	0.1382	−0.0635	4.8
H39	0.4423	0.1903	0.5641	5.2
H40	0.3798	0.1555	0.4689	5.2
H41	0.5444	0.1711	0.5126	5.2
H42	0.7141	0.3340	0.5767	5.5
H43	0.6620	0.4260	0.5760	5.5
H44	0.6116	0.3525	0.6282	5.5
H45	0.4003	0.4098	0.5108	5.3
H46	0.2880	0.3079	0.4672	5.3
H47	0.3539	0.3347	0.5625	5.3

would lower the energy of the d-orbitals available for interaction with the high lying CO* orbitals, diminishing the amount of π-backbonding and causing a shift to higher ν(CO) energy. One must assume rapid interconversion between the two isomers as this "breathing" at ruthenium is silent on the NMR time scale. Other molecules displaying doubling of absorption bands due

to conformational isomers are $Fe(\eta^5\text{-}C_5H_5)(\eta^1\text{-}C_5H_5)(CO)_2$ [21], $Mo(\eta^5\text{-}C_5H_5)(CO)_2C_3H_5$ [22,23], $Fe(\eta^5\text{-}C_5H_5)(CO)_2R$ (R = $PhCH_2$, Et, MeCO) and $Fe(\eta^5\text{-}C_5H_5)(CO)(PPh_3)COMe$ [24]. A single unresolved carbonyl resonance in the $^{13}C\{^1H\}$ MNR is indicative of fluxional pentacoordination geometry, which is ubiquitous for d^8 complexes.

With our continuing interest in the chemistry of $Ru(L)_2(CO)_3$ radical cations in mind, we examined the oxidation of **1** with ferrocenium hexafluorophosphate in CH_2Cl_2. In contrast to other $Ru(L)_2(CO)_3$ (L = Cy_3P, Ph_3P) the radical cation did not abstract a chlorine atom from solvent to give $[Ru(L)_2(CO)_3Cl][PF_6]$. It instead dimerized to give **2**. We have previously noted the apparent tendency of Ru(dppe)$(CO)_3$ (dppe: 1,2-bis(diphenylphosphino)ethane) to dimerize upon oxidation, and the infrared pattern of the dppe dimer is strikingly similar to that of **2** in the ν(CO) region, although the peaks have been shifted to higher energy as expected due to the superior backbonding ability of the bis(phosphite) ligand.

4. Experimental details

4.1. General methods

The preparation and purification of materials were performed under prepurified nitrogen using standard Schlenk-type techniques. The following compounds were purchased and used as received: PCl_3, 2,2′-biphenol, $[NH_4][PF_6]$ from Aldrich; 3-t-butyl-4-hydroxy-anisole from Fluka; $Ru_3(CO)_{12}$ from Strem; Cp_2Fe from Alfa; CO (CP grade) from Matheson. The following were prepared by reported procedures: 1,1′-biphenyl-2,2′-diyl phosphorochloridite, $[Cp_2Fe][PF_6]$. Toluene, hexane, tetrahydrofuran and Et_2O were distilled from sodium benzophenone ketyl. Methylene chloride and Et_3N were distilled from CaH_2. A pale prism crystal of **1** was mounted on a glass fiber and then mounted on an Enraf-Nonius CAD-4 diffractometer. Data collection was carried out with graphite filtered Mo Kα radiation. Infrared spectra were recorded on a Mattson Cygnus 25 FTIR equipped with a HgCdTe detector. ^1H, ^{31}P and ^{13}C NMR were recorded at 300 MHz, 121

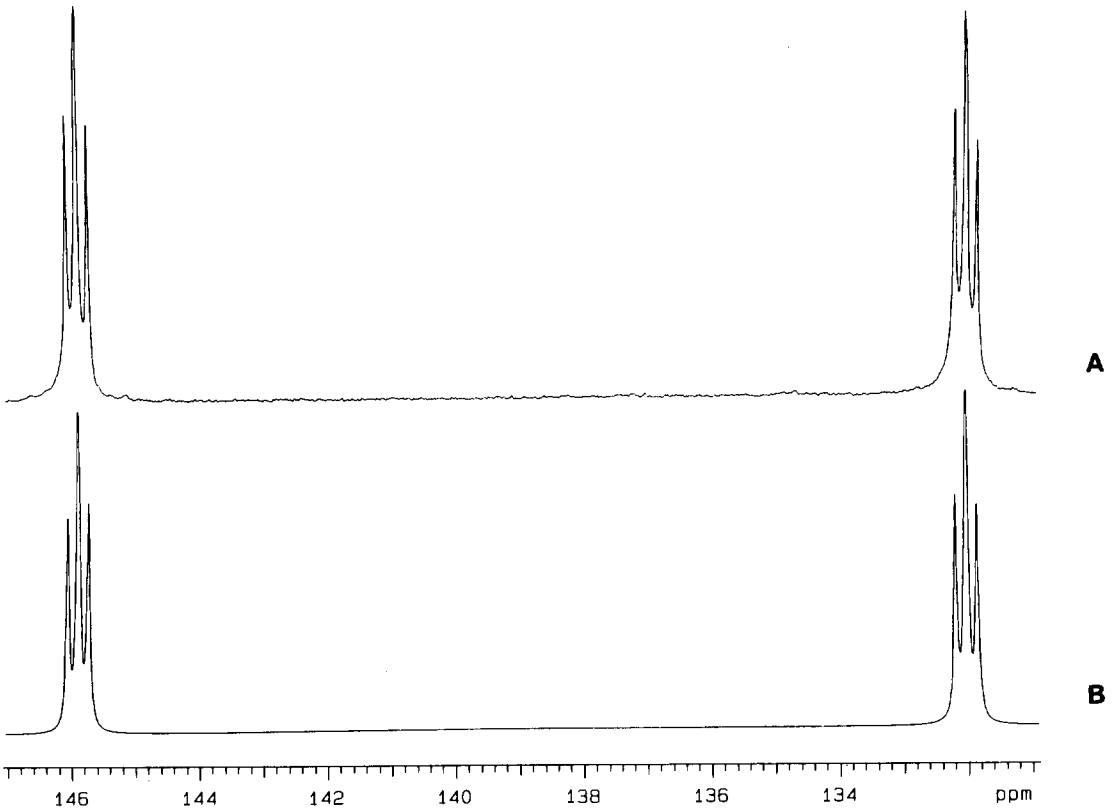

Fig. 3. The observed (A) and calculated (B) $^{31}P\{^1H\}$ NMR spectra for $[(\mu\text{-bbmb})_2Ru_2(CO)_6][PF_6]_2$ (**2**).

MHz and 75 MHz, respectively, on a Varian VXR-300S spectrometer. Chemical shifts are reported in ppm and referenced to residual deuterated solvent signals for ^{1}H and ^{13}C and external 85% H_3PO_4 ($\delta = 0.00$ ppm) for ^{31}P. Ultraviolet spectra were obtained on a HP 8452A diode array spectrometer at various dilutions and ϵ's obtained from Beer's law plots. Low resolution FAB mass spectra were obtained on a VG 7070E-HF instrument. Electrospray mass spectral data was collected using a Sciex API III mas spectrometer (Sciex, Thornhill, Ontario, Canada). The instrument was fitted with a standard pneumatically assisted electrospray atmospheric pressure ionization source. Microanalyses were preformed by M-W-H laboratories. Melting points are uncorrected.

4.2. Synthesis of 3,3'-di-t-butyl-2,2'-dihydroxy-5,5'-dimethoxy-1,1'-biphenyl

A solution of 18.0 g (100 mmol) of 3-t-butyl-4-hydroxyanisole and 11.22 g (200 mmol) of KOH pellets in 34 ml of distilled H_2O was heated at 85°C for 145 min as a stream of compressed air was passed through the solution. The solution was allowed to cool down for only 1–2 min and rapidly filtered leaving a maroon residue. This was washed with 2×50 ml of cold H_2O, 2×5 ml acetone and dried under high vacuum to yield 3.50 g of white powder. The combined H_2O washes along with the original solvent was neutralized to pH ~ 7 using 2.5 M HCl, resulting in the formation of more maroon powder. This was collected, washed with 2×75 ml of H_2O, 2×8 ml of acetone, 3×15 ml of Et_2O and dried under high vacuum to yield an additional 6.52 g (total 10.02 g, 28 mmol, 56%) of white powder. Yields are highly variable and dependent on mixing conditions, air flow rates and reaction times. m.p. 226°C.

4.3. Synthesis of Ru(bbmb)(CO)$_3$ (1)

A 50-ml Parr autoclave was charged with 300 mg (0.47 mmol, 0.016 M) of $Ru_3(CO)_{12}$, 1.11 g (1.41 mmol, 0.047 M) of bbmb and 30 ml of freshly distilled toluene. The autoclave was sealed as expeditiously as possible, purged many times with CO, pressurized to 1120 psi, placed in a heating block, preset at 110°C, and stirred. The final pressure after equilibration (~ 45 min) was 1240 psi. After 24 h, the autoclave was allowed to cool, depressurized and the still effervescent gold solution rapidly transferred to a round bottomed flask, purged with N_2 and the volume of the solution reduced to ~ 5 ml under vacuum. To this was added enough CH_3CN to constitute a homogeneous solution at reflux (~ 80 ml). This was allowed to cool slowly to ambient temperature and stand overnight, depositing 462 mg (0.48

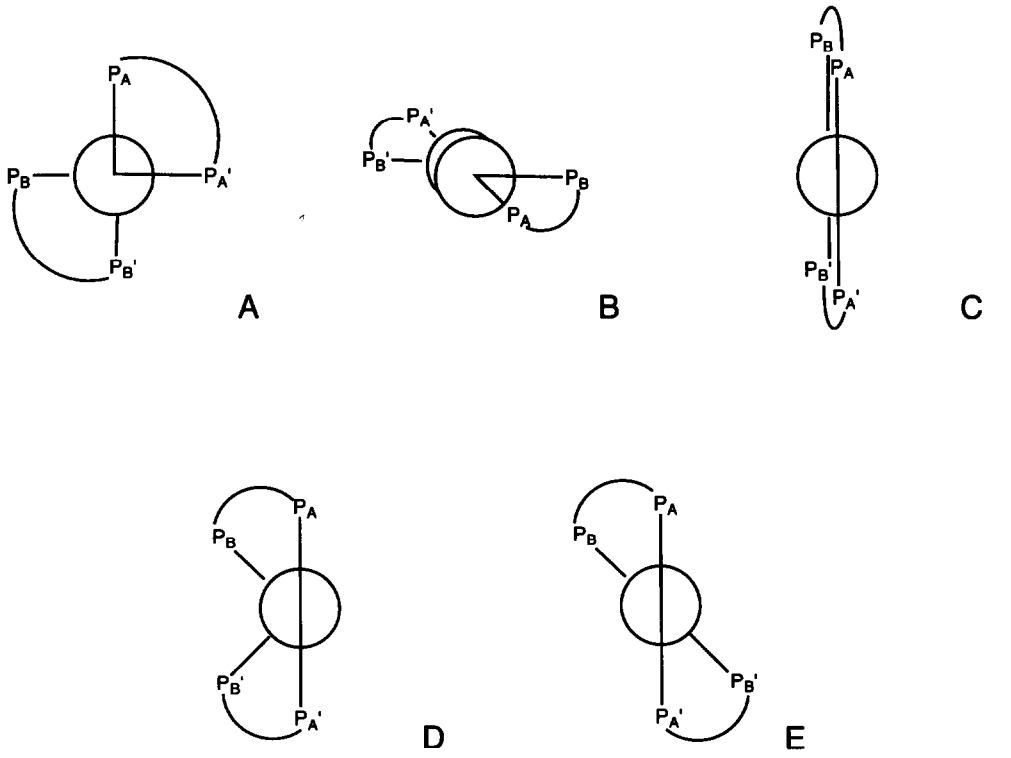

Fig. 4. Structural possibilities for the Ru_2P_4 framework of $[(\mu\text{-bbmb})_2Ru_2(CO)_6][PF_6]_2$ (2).

mmol, 34%) of pale yellow crystals. IR (CH_2Cl_2): ν(CO) 1963s, 1998vs, 2050w, 2069w cm^{-1}, (toluene): ν(CO) 1963s, 1998vs, 2048w, 2068w cm^{-1}; (KBr): ν(CO) 1963s, 1991vs, 2050w, 2065w cm^{-1}. ^1H NMR (C_6D_6): δ 1.52 (s, 18H, $C(CH_3)_3$); 3.39 (s, 6H, OCH_3); 6.8–7.4 (m, 18H, Ar*H*); 7.8 (d, 7.5 Hz, 2H, Ar*H*). $^{31}P\{^1H\}$ NMR ($PhCH_3$): δ 189.4(s). ^{31}C NMR(C_6D_6): δ 207.4 (s, CO). UV (CH_2Cl_2): λ_{max} = 238 nm (ϵ = 46,673 M^{-1} cm^{-1}). FAB/MS (*m/e*): $Ru(bbmb)(CO)_3^+$, 973; $Ru(bbmb)(CO)_3^+ - n$ CO (n = 1–3), 944, 917, 888. m.p.(sealed/N_2) decomposes 218–220°C. Anal. Found: C, 60.56; H, 4.80; P, 6.53. $Ru(bbmb)(CO)_3$ calcd: C, 60.56; H, 4.56; P, 6.37%.

4.4. X-ray crystallography of $Ru(bbmb)(CO)_3$ (1)

Pale yellow prisms were grown by slow diffusion of hexane onto a toluene solution and one of these was mounted on a glass fiber. Table 1 includes the details of the structural analysis. A preliminary peak search of 25 centered reflections ($12° < 2\theta < 38.2°$) indicated that the crystal was triclinic. The TEXSAN programs used for the least-squares refinement incorporated the estimated standard deviations of the cell parameters in the calculation of the errors in bond distances and angles. The centric space group $P\bar{1}$ (No. 2) was chosen and led to successful refinement of the structure. During data collection, no decay of intensity was observed in three check reflections measured every 50 min. All non-hydrogen atoms, except C48 and C49, were refined anisotropically. The carbon atom attached to O42 was disordered over two locations labelled C48 and C49. The refined occupancies were 0.555(5) and 0.445(5), respectively. The thermal parameters for both atom locations were refined isotropically. Hydrogen atoms were included in the structure factor calculation in idealized positions with $d_{(C-H)}$ = 0.95 Å and an isotropic temperature factor 20% greater than B_{eq} of the carbon to which they were bonded. The maximum and minimum peaks on the final difference Fourier map correspond to +1.11 and −1.35 e $Å^{-3}$, respectively. The values of the atom scattering factors used in the calculations were taken from the usual tabulations, and the effects for anomalous dispersion were included for the non-hydrogen atoms [24–26]. The bond distances and bond angles are listed in Tables 2 and 3. Figure 1 shows the molecular structure of **1**.

4.5. Synthesis of $[Ru_2(\mu\text{-bbmb})_2(CO)_6][PF_6]_2$ (2)

Finely powdered $[Cp_2Fe][PF_6]$ (136 mg, 0.41 mmol), was added all at once, from a dip tube, to 400 mg (0.41 mmol, 0.027 M) of **1** in 15 ml of freshly distilled CH_2Cl_2. The initial pale yellow solution turned forest green upon addition of the oxidant and the solution slowly turned yellow after ~25 min. After 2.5 h at ambient temperature, the yellow solution was transferred, *via* cannula, to a round-bottomed flask attached to a reversible frit (D). Solvent was removed, the residue washed with 2 × 10 ml of toluene and 6 ml of THF, recrystallized twice from 1:10 CH_2Cl_2/toluene, washed with 2 × 10 ml of hexane and dried under high vacuum to yield 178 mg (0.08 mmol, 39%) of canary yellow microcrystalline **2**. IR (CH_2Cl_2): ν(CO) 2053m, 2063vs, 2078vs, 2098m, 2101m, 2134w cm^{-1}; (KBr): ν(CO) 1963brw, 1996w (**1**), 2058s, 2075vs, 2098m (**2**), 2142w cm^{-1}. ^1H NMR (CD_2Cl_2): δ 1.63 (s, 9H, $C(CH_3)_3$); 1.63 (s, 9H, $C(CH_3)_3$); 3.25 (s, 3H, OCH_3); 3.60 (s, 3H, OCH_3); 6.0–8.0 (m, 20H, Ar*H*). $^{31}P\{^1H\}$ NMR (CD_2Cl_2): δ 132.1 (t, 21.5 Hz), 146.0 (t, 21.5 Hz), −143.0 (h, J_{PF} = 708 Hz, PF_6^-). ^{13}C NMR (CD_2Cl_2): δ 194 (brs, CO). UV (CH_2Cl_2): λ_{max} = 236 nm (ϵ = 42,700 M^{-1} cm^{-1}); λ = 388 nm (ϵ = 13,900 M^{-1} cm^{-1}). ES/MS (*m/e*): $\{[Ru_2(\mu\text{-bbmb})_2(CO)_6][PF_6]\}^+$, 2089; $[Ru_2(\mu\text{-bbmb})_2(CO)_6]^{+2} - n$ CO (n = 1–3), 944, 916, 888. FAB/MS (*m/e*): $[Ru_2(\mu\text{-bbmb})_2(CO)_6]^{+2}$, 972; $[Ru_2(\mu\text{-bbmb})_2(CO)_6]^{+2} - n$ CO (n = 1–3), 944, 917, 888. m.p.(sealed/N_2) decomposes > 200°C. Anal. Found: C, 52.51; H, 4.04; P, 8.48. $[Ru_2(\mu\text{-bbmb})_2(CO)_6][PF_6]_2$ calcd: C, 52.69; H, 3.97; P, 8.32%.

Acknowledgment

The research was supported by a grant from the National Science Foundation (CHE-9223433).

References

1 L.H. Pignolet (ed.), *Homogeneous Catalysis with Metal Phosphine Complexes*, Plenum, New York, 1983.
2 E. Billig, A.G. Abatjoglou and D.R. Bryant, Union Carbide, *US Pat. 4,769,498*, 1988.
3 M.J. Baker, K.N. Harrison, A.G. Orpen, P.G. Pringle and G. Shaw, *J. Chem. Soc., Chem. Commun.*, (1991) 803.
4 M.J. Baker and P.G. Pringle, *J. Chem. Soc., Chem. Commun.*, (1991) 1292.
5 T.V. RajanBabu and A.L. Casalnuovo, *J. Am. Chem. Soc., 114* (1992) 6265.
6 J.D. Gargulak, M.D. Noirot and W.L. Gladfelter, *J. Am. Chem. Soc., 113* (1991) 1054.
7 J.D. Gargulak, A.J. Berry, M.D. Noirot and W.L. Gladfelter, *J. Am. Chem. Soc., 114* (1992) 8933.
8 S.J. Sherlock, D.C. Boyd, B. Moasser and W.L. Gladfelter, *Inorg. Chem., 30* (1991) 3626.
9 D.R. Tyler, R.A. Levenson and H.B. Gray, *J. Am. Chem. Soc., 100* (1978) 7888.
10 H.B. Abrahamson, M.C. Palazzotto, C.L. Reichel and M.S. Wrighton, *J. Am. Chem. Soc., 101* (1979) 4123.
11 K.P.C. Vollhardt and T.W. Weidman, *J. Am. Chem. Soc., 105* (1983) 1676.
12 L. Song and W.C. Trogler, *J. Am. Chem. Soc., 114* (1992) 3355.
13 J.R. Bleeke, A.J. Donaldson and W-J. Peng, *Organometallics, 7* (1988) 33.

14 G.M. Gray, F.P. Fish, D.K. Srivastava, A. Varshney, M.J. van der Woerd and S.E. Ealick, *J. Organomet. Chem.*, *385* (1990) 49.
15 C.P. Casey and G.T. Whiteker, *Isr. J. Chem.*, *3* (1990) 299.
16 C.P. Casey and G.T. Whiteker, *J. Org. Chem.*, *55* (1990) 1394.
17 C.P. Casey, G.T. Whiteker, C.F. Campana and D.R. Powell, *Inorg. Chem.*, *29* (1990) 3376.
18 C.P. Casey, G.T. Whiteker, M.G. Melville, L.M. Petrovich, J.A. Gavney, Jr. and D.R. Powell, *J. Am. Chem. Soc.*, *114* (1992) 5535.
19 J.L. Graff, R.D. Sanner and M.S. Wrighton, *Organometallics*, *1* (1982) 837.
20 A.R. Rossi and R. Hoffmann, *Inorg. Chem.*, *14* (1975) 365.
21 F.A. Cotton and T.J. Marks, *J. Am. Chem. Soc.*, *91* (1969) 7523.
22 R.B. King, *Inorg. Chem.*, *5* (1966) 2242.
23 A. Davison and W.C. Rode, *Inorg. Chem.*, *6* (1967) 2124.
24 S.C. Mackie, Y-S. Park, H.F. Shurvell and M.C. Baird, *Organometallics*, *10* (1991) 2993.
25 D.T. Cromer and J.T. Waber, *International Tables for X-ray Crystallography*, Vol. 4, The Kynoch Press, Birmingham, 1974, Table 2.2A.
26 J.A. Ibers and W.C. Hamilton, *Acta Crystallogr.*, *17* (1964) 781.
27 D.T. Cromer, *International Tables for X-ray Crystallograhy*, Vol. 4, The Kynoch Press, Birmingham, 1974, Table 2.3.1.